On the Feasibility of URLLC for 5G-NR V2X Sidelink Communication at 5.9 GHz

Jin Yan, Jérôme Härri

On the Feasibility of URLLC for 5G-NR V2X Sidelink Communication at 5.9 GHz

Jin Yan, Jérôme Härri

EURECOM, 450 route des Chappes, 06904 Sophia-Antipolis, France

E-mail: {jin.yan,jerome.haerri}@eurecom.fr

***Abstract*—Delivering ultra-reliable low-latency communication (URLLC) services on 5G New Radio (NR) is critical for extended Vehicle-to-everything (V2X) applications. Early studies focused either on infrastructure V2X communications, or exclusively evaluating performance on mmWave band, but never so far for V2X Sidelink communications. In this paper, we evaluate the feasibility of achieving URLLC critical requirements for 5G NR V2X Sidelink communication at the V2X 5.9 GHz band. We propose a higher 5G-NR numerology completed by a deterministic scheduler and propose an analytical V2X SL admission control algorithm to reach tight URLLC requirements.**

I. Introduction

With the continuous rapid development of new innovative Vehicle-to-Everything (V2X) services requiring higher data volumes and reliability, 5G New Radio (NR) V2X has been designed to provide enhanced communication capabilities either on Uplink/Downlink (Uu) or on Slidelink (SL) 5G-NR interfaces. However, some promising services require V2X performance beyond the current 5G-NR V2X capabilities specified by 3GPP rel. 16 [1]. In particular, Ultra-Reliable Low Latency Communication (URLLC) is expected to be critical for highly innovative V2X services, such as tele-operated driving, platooning or industrial robotics. If specifications for 5G NR URLLC are due for rel.16, 5G NR V2X URLLC is not expected to be available before rel.18-19 at the earliest[1].

A large number of studies are available on innovations and enablers for 5G NR URLLC as described and referenced by Ali et. al [2], proposing various strategies to improve reliability. To address latency constraints, a typical approach in 5G NR development is to use a higher numerology in order to reduce the duration of transmission time intervals (TTI) (e.g. [3]), which may however interfere with other parts of the spectrum under different numerologies. Zambianco et al. [4] investigated Inter-Numerology Interference (INI) between eMBB and URLLC slices and proposed using a deep reinforcement learning agent to mitigate INI.

Only few studies are available for 5G NR V2X. Feng et al. [5] suggests multiple methods of centralised Cloud management, such as Mobile Edge Computing (MEC), or assignment by road-side units (RSUs). Another study by Ge et al. [6] proposes a monte-carlo approach to tackle a combined optimization of reliability and latency for URLLC V2X on the millimeter wave band (FR2). These studies do not, however, consider the use of Sidelink (SL) communication or the sub-6GHz band (FR1), including the C-ITS band at 5.9GHz.

In this paper, we evaluate the feasibility and network configurations enabling URLLC performance for 5G NR V2X SL at 5.9GHz. Our contributions are as follows: (i) we evaluate the impact of the 5G NR numerology-3 in FR1 providing 0.125ms TTI, (ii) we propose and evaluate the performance of a deterministic scheduler based on orthogonal optical codes (OOC) [7] to guarantee delay bounds, (iii) we introduce an admission control mechanism restricting the number of V2X UE (VUE) to guarantee URLLC requirements. This paper provides a holistic study to evaluate the conditions under which URLLC may be supported. These conditions may later be considered as the operational mechanisms required to operate a 5G NR V2X SL URLLC slice for future stringent enhanced V2X services.

The rest of the paper is organized as follows: Section II provides background on 5G NR V2X and URLLC. Section III describes the methodology used in this study, while Section IV provides evaluation results. Section V summarizes the key findings.

II. Background & State-of-Art

A. 5G NR Sidelink in V2X Communication

Sidelink (SL) is an extension of 5G NR communication [1] to support device-to-device (D2D) communication. Defined in 3GPP since LTE rel. 12 for Proximity Services (ProSe), SL has been specified for 5G NR in rel. 16 for V2X communication. Further releases (rel.17 and 18) define SL enhancements, aiming to support more stringent requirements and operation scenarios for V2X or ProSe, such as wider coverage, reliability improvement, latency reduction or power. More detailed information can be found on 5G NR V2X in Garcia et al. [1].

5G NR SL V2X physical resources are similar to 5G NR and span across time and frequency domains. In the frequency domain, the bandwidth is split into 15kHz Physical Resource Blocks (PRB). In the time domain, a 10 ms frame is divided into 10 sub-frames, which are further divided into numerous *mini-slots*.

Contrary to fixed sub-carrier spacing in C-V2X, 5G NR supports a flexible frame structure with reduced transmission

[1]source: 3GPP WI NR_SL_enh2 Rel.18 and beyond.

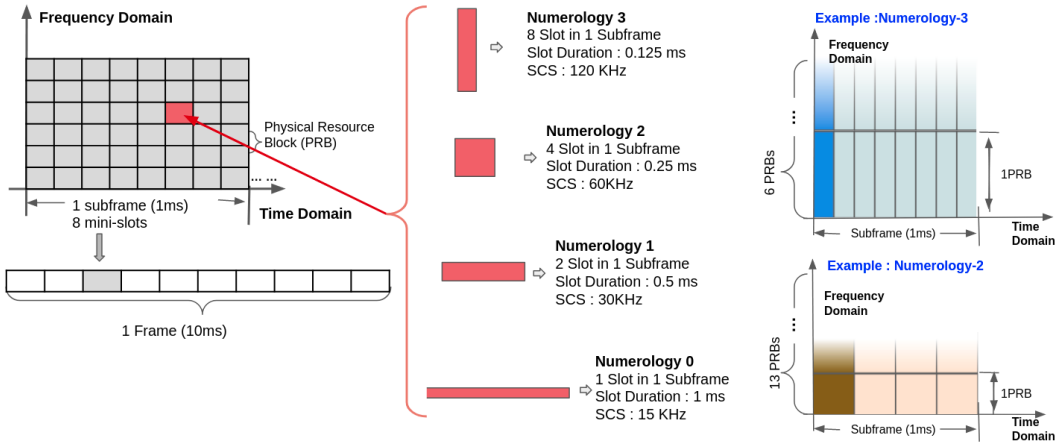

Figure 1: 5G NR Sidelink Physical Numerology

time intervals (TTI), which are equal to the *mini-slot* duration. The TTI can be reduced from 1 ms (under numerology-0) to 0.125 ms (under numerology-3). Keeping the number of resources per slot equal, mini-slots proportionally increase the required frequency resources as depicted in Fig. 1. Accordingly, the number of slots available per 5G NR sub-frame varies according to the applied numerology.

Two MAC layer scheduling modes - mode 1 (infrastructure supported) and mode 2 (ad-hoc) - are available for 5G NR V2X SL communication. In mode 2, four enhanced sub-modes are further defined (as depicted in Fig. 2): in 2(a), each vehicle can select its resources autonomously based on semi-persistence sensing-based scheduling; 2(b) is a cooperative distributed scheduling approach, where UEs can assist each other in resource selection, for instance by sharing their selection window with neighboring VUEs and mitigating near-far effects; in 2(c), a VUE assigns resources for others based on (pre-)configured transmission patterns; in 2(d), a VUE schedules the SL transmissions for its neighbouring VUEs. As can be seen from Fig. 2, mode 2(a), corresponding to the default scheduling mode for 5G-NR V2X SL, does not provide any delay bound and if mode 2(b) improves reliability, it cannot provide any delay bound neither. However, modes 2(c) and 2(d) correspond to deterministic scheduling options and accordingly are expected to be prime candidates for URLLC.

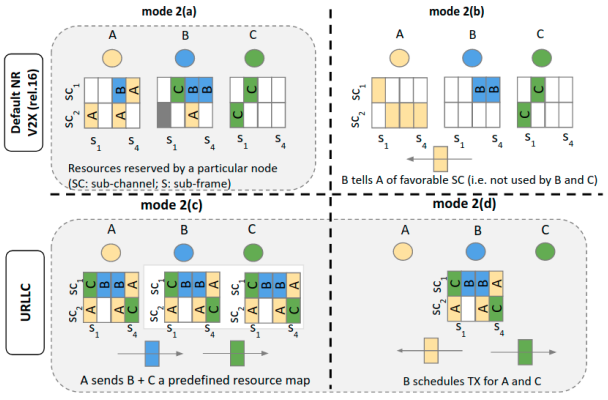

Figure 2: Scheduling sub-modes for 5G NR V2X SL

B. URLLC Service in 5G-NR V2X Communication

URLLC is defined in two aspects : reliability/delay requirements and specific traffic patterns. 3GPP rel.17 [8] defines URLLC as providing a 10^{-5} reception reliability with a 1 ms delay for 32-byte packets. 3GPP considers adapted requirements for 5G-NR V2X SL as 10^{-5} reception reliability with 3-10 ms delay for 300-byte packets.

3GPP does not provide details on how the delay should be distributed between 3-10 ms. A more suitable formulation requires defining a reliability level of the expected delay. For example, a 4 ms delay with reliability 10^{-5} (i.e. a prob. 10^{-5} for the delay to exceed 4 ms). Accordingly, we define in this paper V2X URLLC in the following terms: reception reliability of 10^{-x} and a y ms delay with reliability of 10^{-z}. Evaluating 5G NR V2X capabilities to provide URLLC will require that we identify the x, y and z parameters. In particular, we will focus less on a given delay value but rather on the reliability of that delay value.

V2X traffic patterns for URLLC services are expected to be significantly different from regular (awareness) services, because they involve smaller data packets, a smaller transmit range and fewer users. Default 5G NR V2X SL parameters (numerology, sub-channels, MAC protocol, etc.) therefore need to be changed to adjust to such specific traffic patterns.

Finally, as previously described, most URLLC studies for 5G-NR V2X consider a FR2 spectrum (mmWAVE) and, to the best of our knowledge, none consider SL. As various extended V2X (eV2X) services with URLLC requirements focus on SL communication at 5.9GHz (FR1), we specifically focused on it in this paper. V2X SL URLLC at 5.9GHz is challenging to meet. First, only 10 or 20 MHz of bandwidth is reserved for V2X communication, which might be insufficient if a higher numerology is involved [9].

Second, the eV2X services cannot rely on the full availability of a 5GS infrastructure, and the default 5G-NR V2X SL mode 2 scheduler does not support time-deterministic channel access time.

C. 5G NR V2X Admission Control for URLLC

URLLC services have specific traffic patterns and in exchange, V2X URLLC services need to meet extreme reliability and delay requirements. In the current rel. 16 specification, 5G-NR V2X SL mode 2 is designed to admit any VUE, although its performance quickly degrades as a function of the number of VUEs [1]. URLLC QoS cannot be met under unrestricted access policy, and a robust admission control strategy is required to accept the optimal number of VUEs for which stringent requirements can be met.

Admission control defines maximum users that can be admitted simultaneously to the system while efficiently using the available resources and satisfying QoS requirements. Admission control is therefore central to any 5G systems and more specifically to optimizing 5G NR slices (enhanced Massive Broadband (eMBB), massive Machine-Type Communication (mMTC) or URLLC).

Shashika et al. [10] proposed an optimization algorithm to tackle admission control optimization in a Multiple-Input Single-Output system. In [11], Ginige et al. proposed a coexistence support for both eMBB and URLLC users in 5G-NR, and pointed out the necessity of controlling the admissions of eMBB users to facilitate scheduling for all URLLC users.

3GPP so far does not describe admission control strategies for 5G-NR V2X SL mode 2 slices. In this paper, we evaluate the optimal number of users that can be admitted into a 5G-NR V2X SL URLLC slice, consisting of a NR numerology-3 and a dedicated mode 2(c) scheduler, and guaranteeing URLLC QoS requirements.

III. Methodology

In this section, we describe the three blocks required for 5G-NR V2X SL URLLC : higher physical layer numerology, a deterministic scheduler and URLLC admission control.

A. Physical Resource Arrangement in 5G NR

Since a higher numerology can effectively reduce the duration of a *mini-slot*, which is compensated for by its expansion of the frequency domain, we therefore apply numerology-3, which enables a unit duration as small as 0.125 ms. Considering the limited V2X bandwidth in 5.9 GHz frequency, in order to meet the 300 bytes packet size specified for URLLC SL from [8], and to avoid the half-duplexing problem, we consider a pure time-domain multiplexing. As depicted in the right-hand image in Fig 1, considering a 10 MHz assigned V2X bandwidth under numerology-3, all 6 available PRBs are uniformly assigned to one user[2].

Two Modulation and Coding Scheme (MCS) values are investigated: MCS-8 (1/2 QPSK), which is the default V2X modulation to achieve a data rate of 6 Mbps; MCS-24 (64 QAM), which provides a better overall performance as described in [12] for numerology-0. The maximum capacity S^M supported per allocation unit (i.e one *mini-slot*) can be approximately evaluated based on Eq. 1.

[2]Although 20 MHz is also baseline of bandwidth assigned for 5G NR V2X communication, this is left for future study.

$$S^M = 1/8 \times CR \times Q^m \times N^{Sym} \times N^{PRB} \times N^{sub} - S^h \quad (1)$$

We addressed two MCS impact factors : effective code rate value (CR) and modulation order (Q_m), which are described in Tables 5.1.3.1-2 in 3GPP standard [13]. N^{sym} represents the available symbols per slot for V2X traffic load (we consider 8 out of 14 symbols), N^{PRB} indicates the total available number of PRB in the frequency domain, N^{sub} indicates the number of subcarriers per slot, which is fixed to 12, and finally S^h is a 3-byte reservation for CRC_Length.

The maximum capacity under different numerology values calculated based on Eq. 1 is listed in Table I. Focusing on numerology-3 and a mini-slot of 0.125 ms, MCS-24 has a capacity capable of supporting V2X standard 300-byte packets. Yet at a lower modulation MCS-8, 32-byte packets can still be handled. We conclude that although numerology-3 is not defined for FR1 (5.9GHz) by 3GPP, it can significantly improve latency while offering sufficient traffic capacity, even with a 10 MHz V2X bandwidth.

μ	**mini-slot**	**MCS-8**		**MCS-24**	
	Size(ms)	$\mathbf{N^{PRB}}$	$\mathbf{S^M}$(bytes)	$\mathbf{N^{PRB}}$	$\mathbf{S^M}$(bytes)
0	1	53	736.2	53	2848.7
1	0.5	26	361.1	26	1397.5
2	0.25	13	180.6	13	698.8
3	0.125	6	83.3	6	322.5

Table I: Max Capacity of one $mini-slot$

B. Deterministic Scheduler Design

According to Section II-A, mode 2(c) and 2(d) enable potential scheduling strategies suitable for URLLC services. In this paper, we propose an Optical Orthogonal Code (OOC)-based deterministic mode-2(c) scheduler supporting channel access delay bounds. OOC has been adapted to a variety of channel access technologies, in particular by Gallo et al. [14] for C-V2X. This technique improves delivery reliability by restraining the maximum cross-correlation between binary code-words among any pairs of codewords v, u, as described in Eq. 2. The OOC-based deterministic scheduling procedure is listed below.

$$\sum_{j=1}^{L} v_j \cdot u_j \leq \lambda \qquad \forall u \neq v \quad (2)$$

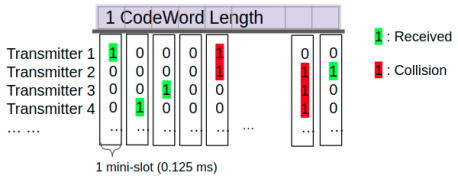

Figure 3: Example of OOC Access

- A L-bit long OOC codewords transmission pattern is pre-configured while satisfying the cross-correlation constraint condition. Each bit is associated with one *mini-slot* (duration of 0.125 ms).

- VUEs can transmit a packet in a *mini-slot* when the corresponding OOC indicator is 1-bit; VUEs switch to receiving mode while the OOC indicator is 0-bit.
- The transmission status is illustrated in Fig. 3, where red 1-bits refer to transmission collisions while green 1-bits indicate successful, collision-free receptions.
- w decides re-transmission rate, which corresponds to the total number of 1-bits within one code-word.

C. URLLC V2X SL Admission Control Mechanism

URLLC services require to restrict access to a limited number of users. To analyse such limit, the maximum capacity for the accessible VUE needs to be analyzed. We formulate the admission control problem into an optimization equation in Eq. (3). The binary array $K(i)$ indicates whether SL link i meets both reliability and latency demands, as expressed in Eq. (4), therefore the optimal target is to maximize SL access link connections, indicating maximum system capacity.

$$\begin{aligned} \max_{w,L,N} \quad & \sum_{i=1}^{N} k(i) \\ \text{s.t.} \quad & P_e \leq 10^{-5} \\ & P_{T_d} \leq P_t^{min} \\ & L \in [0, 150], \forall L \in \mathbb{Z}^+ \end{aligned} \tag{3}$$

$$k(i) = \begin{cases} 1 & \text{if } P_e \leq 10^{-5}, \text{ and } P_{T_d} \leq P_t^{min} \\ 0 & \text{otherwise.} \end{cases} \tag{4}$$

Constraints for the optimization problem relate to both reliability and latency URLLC service requirements. We focus on a reception reliability P_e of 10^{-5}, and a T_d ms delay with reliability of P_t^{min}. P_e is expressed in Eq. (5), as a function of the probability of success reception P_{sw} of one transmit packet over w transmission attempts.

In this study, λ is set to 1 so that every pair of codewords can have at most one overlapping '1'. μ represents transmission probability which is set to '1'. A uniform random access selection is considered, therefore Eq. (6) can be simplified as $P^*_{s_w}$. Moreover P_{T_d} is defined in Eq. (8).

$$P_e = (1 - P_{s_w})^w \tag{5}$$

$$P_{s_w} = \mu \frac{\binom{L-w}{w-j}}{\sum_{l=0}^{\lambda} \binom{w}{l}\binom{L-w}{w-l}} \tag{6}$$

$$P^*_{s_w} = (1 - \frac{w}{L})^{N-1} \tag{7}$$

$$P_{T_d} = P^*_{s_w} + \sum_{i=0}^{\lceil \frac{T_d \times 8 \times W}{L} \rceil} w/L \times P^*_{s_w} \times (1 - P^*_{s_w})^i \tag{8}$$

We can see that L and w have cost-benefit trade-offs on both P_e and P_{T_d} performance: longer OOC codes L are capable of guaranteeing more admitted SL links, but are inclined to allocate re-transmission slots separately, which significantly increases delay. Moreover, longer OOC codes reduce the system efficiency, particularly for periodical connections, which is relevant to URLLC service. Higher values for w promise a higher probability of successful reception, however resource exhaustion is reached more quickly.

The process of solving this admission control optimization is described in Algorithm 1, which provides the maximum number of SL users that can be admitted under each L.

Algorithm 1 Admission Control Algorithm

```
while w < 4 do
    while N < N^max do
        i ← N
        if P_e ≤ 10^-5 and P_Td ≤ P_t^min then
            k(i) ← 1
        else
            k(i) ← 0
        end if
        N ← N + 1
    end while
    return K*_w(N) = Σ_{i=1}^{N} k(i)
    w ← w + 1
end while
```

IV. Evaluation

A. Simulation Environment and KPI

The mechanisms described in Section III are evaluated by Matlab simulations according to parameter settings described in Table II. All vehicles are allocated on a one-lane road scenario sending messages in broadcast to one reception vehicle[3]. A configurable number of transmitters are randomly generated according to the target 1km-wide communication density. Analysis of the impact created by channel fading, phase shifting and other physical layer criteria is left for future studies. Data traffic is generated at 10 Hz (100 ms) over the total simulation time to allow an ergodic analysis.

Table II: Simulation Parameters Setting

Parameter	Value
Bandwidth	10 MHz
Applied Numerology	3
Hamming Weight w	1,2,3,4
Transmission Range	1000 m
Packet Rate	100 ms
Simulation time	30 ms
Runs	300

Three key performance indicators (KPI) are selected in this paper:

- *Packet Reception Rate (PRR)* : This parameter is expressed in a Complementary Cumulative Distribution Function (CCDF) in relation to the number of transmitters.
- *Delay* : Delay is considered from two dimensions as depicted in Fig 4: the *absolute delay* measures the time interval from the generated data packet; the *relative delay* only considers the exact air time including channel access delay. Without re-transmission, this value is set to one mini-slot (0.125 ms), whereas with re-transmissions this value is calculated as the time between the first successful reception and the relative starting time.
- *Number of controlled admissions* : This indicates the maximum number of admitted V2V (SL) links when both

[3]The broadcast transmission is intended to all vehicles, but we only consider 1 receiving vehicle for analysis purpose.

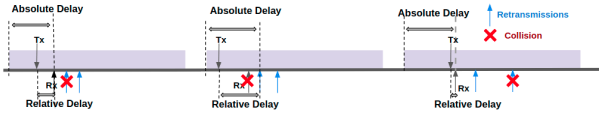

Figure 4: Delay Illustration

the packet reception rate and the delay conditions are satisfied.

B. Performance Analysis under a fixed L

In this section we investigate the performance regarding PRR and delay criteria under a fixed code-length of $L = 90 \times 8$. Moreover, we focus on the most strict sub-ms (< 1ms) latency requirement depicted in Fig 5. Comparison between analytical (in dashed points) and simulation results (in bold lines) are indicated in both figures.

Overall the PRR and delay reliability both decrease as the number of admitted users increases. The analytical model over-estimates the optimal number of admitted users, as the simulation results are subject to near-far issues, where additional collisions occur from out-of-coverage users, reducing the number of admitted users.

In a higher-density scenario, near-far characteristics results in a greater impact, consequently the difference between the analytical and simulation results widens. We therefore may consider the analytical model as an optimal benchmark.

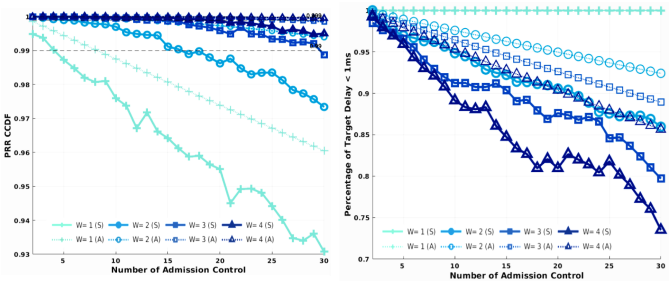

(a) PRR ccdf distribution (b) Probability (Delay $\leq$ 1ms)

Figure 5: PRR and Delay Distribution Graph of $L = 90 \times 8$

Nevertheless, we may observe correlated relationships between the analytical model and simulations under different re-transmission time w values: firstly a higher w can effectively improve the overall reliability suggested in Fig. 5a, we can also verify that with lower $w = 1, 2$, it is extremely difficult to achieve the target reliability demand; secondly in terms of latency depicted in Fig. 5b, as additional re-transmissions produce higher delays, the probability of fulfilling the sub-ms latency requirement is considerably reduced when more re-transmissions are generated. We can therefore identify that $w = 3$ achieved the optimal number of users admitted under the target URLLC requirement.

Examining the absolute delay in more depth via simulations, Fig. 6 depicts the distribution of the absolute delay, as we are interested in estimating the probability of a user being admitted under a given delay threshold. Accordingly, we rely on a kernel density estimate providing an overall evaluation of various distribution tendencies. It can be observed that the number of peaks for certain delay values is correlated with w, each peak representing the average delay of a transmission event.

A comparison between different traffic densities is made between 5 transmitters on Fig. 6a and 20 transmitters on Fig. 6b. With fewer transmitters, the delay values are more closely packed at the beginning; however, with increasing transmitters, there is a higher probability of collision at the first transmission, and success reception events are spread sporadically over time, which leads to a higher delay. Higher w values also perform better under sparse scenario, but when traffic increases, there is a higher chance of collision at the first transmission.

We can conclude that if the proposed OOC mode 2(c) scheduler provides efficient URLLC performance in specific scenarios, codewords with additional dynamic correlation properties will need to be studied to better adapt to different scenarios.

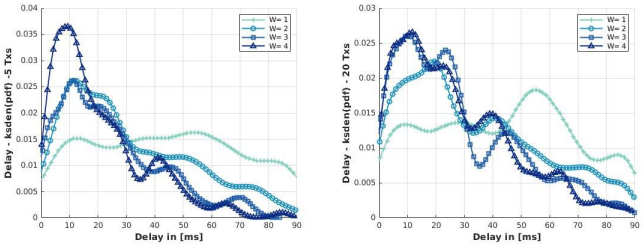

(a) 5 Transmitters (b) 20 Transmitters

Figure 6: Absolute Delay of $L = 90 \times 8$

C. General Result Analysis

In this Section, we generalize this study using a wider range of codeword lengths, and summarize results in Table III. Note that lower w values can only support an extremely limited number of SL links under URLLC requirements. We therefore only focus on $w = 3$ and $w = 4$.

Without loss of generality, we conduct simulations with a codeword length of $[8 \times 60,\ 8 \times 120]$ (60, 120 indicating length in ms) to evaluate if an optimal codeword length can be identified. Considering L, the lower bound is the minimal requirement to support at least 2 transmitters to meet the target reliability constraint, whilst the upper bound is designed to limit one transmission per link within one frame.

$A - Result$ values are obtained from analytical model while $S - Result$ values are produced from simulations from scenarios described in Section IV-A.

N^* represents the maximum supported SL links to meet the target reliability P_e of 10^{-5}, while $P_{Td} \leq 1ms$ gives the corresponding probability for a successful reception within 1 ms latency. Again, the analytical results generally overestimate the simulation results, due to simulation randomness and the aforementioned near-far problem.

With higher w both analytical and simulation results show correlated benefits maximizing the supported admission SL links. However, the relative delay increases, and the benefit is accordingly not significant enough to justify an increase from $w = 3$ to $w = 4$, or higher. Overall with $w = 3$ and an optimal code-word length ranging from $[8 \times 90,\ 8 \times 95]$,

Index		Code Length L	60×8	70×8	80×8	85×8	90×8	95×8	100×8	110×8	120×8
$\mathbf{w=3}$	A-Result	$\mathbf{N^*}$	8	9	11	11	12	13	13	14	16
		$\mathbf{P_{Td}\leq 1ms}$	0.9591	0.9596	0.9557	0.9582	0.9565	0.9550	0.9571	0.9577	0.9552
	S-Result	$\mathbf{N^*}$	2	3	4	4	6	6	5	7	8
		$\mathbf{P_{Td}\leq 1ms}$	0.92	0.971	0.964	0.97	0.947	0.962	0.985	0.956	0.959
		$\mathbf{P_t^{min}\leq 0.9}$	$\leq 1ms$	$\leq 1ms$	$\leq 1ms$	$\leq 1ms$	$\leq 1ms$	$\leq 1ms$	$\leq 1ms$	$\leq 1ms$	$\leq 1ms$
		$\mathbf{P_t^{min}\leq 0.99}$	$\leq 30ms$	$\leq 30ms$	$\leq 35ms$	$\leq 35ms$	$\leq 35ms$	$\leq 40ms$	$\leq 10ms$	$\leq 30ms$	$\leq 50ms$
		$\mathbf{P_t^{min}\leq 0.999}$	$\leq 40ms$	$\leq 45ms$	$\leq 70ms$	$\leq 60ms$	$\leq 80ms$	$\leq 70ms$	$\leq 40ms$	$\leq 90ms$	$\leq 95ms$
$\mathbf{w=4}$	A-Result	$\mathbf{N^*}$	13	15	17	18	19	20	22	24	26
		$\mathbf{P_{Td}\leq 1ms}$	0.9102	0.9094	0.9088	0.9086	0.9084	0.9082	0.9036	0.9037	0.9037
	S-Result	$\mathbf{N^*}$	5	7	8	8	7	6	12	13	14
		$\mathbf{P_{Td}\leq 1ms}$	0.932	0.906	0.915	0.909	0.934	0.922	0.886	0.909	0.892
		$\mathbf{P_t^{min}\leq 0.9}$	$\leq 1ms$	$\leq 1ms$	$\leq 1ms$	$\leq 1ms$	$\leq 1ms$	$\leq 1ms$	$\leq 5ms$	$\leq 1ms$	$\leq 5ms$
		$\mathbf{P_t^{min}\leq 0.99}$	$\leq 30ms$	$\leq 40ms$	$\leq 40ms$	$\leq 30ms$	$\leq 40ms$	$\leq 50ms$	$\leq 45ms$	$\leq 50ms$	$\leq 55ms$
		$\mathbf{P_t^{min}\leq 0.999}$	$\leq 40ms$	$\leq 55ms$	$\leq 60ms$	$\leq 45ms$	$\leq 65ms$	$\leq 70ms$	$\leq 75ms$	$\leq 80ms$	$\leq 90ms$

Table III: General Result under different Code-word Length

the investigated 5G-NR V2X SL URLLC slice may support approximately 6 users.

It must be noted that this study is based on a worst-case scenario, only considering absolute collisions, and ignoring mobility, which has a favorable impact on fading and channel coding that could mitigate the number of packet losses. It is therefore possible to expect a better performance under more realistic conditions, which we plan for future work.

The reliability of a given delay to be met is also listed in Table III, with relative delay threshold P_t^{min} of 99%, 99.9% and 99.99% (i.e. 10^{-1}, 10^{-2} and 10^{-3} failure for exceeding the target delay). Although some of the delay times are excessively long, this can still be considered a positive result, as it shows that 5G NR V2X SL at 5.9Ghz with 10Mhz bandwidth may provide a 10^{-4} reception reliability and a 10^{-1} delay reliability lower than 1 ms. Such reliability is better than what can be provided by the current 5G NR V2X SL communication systems.

V. Conclusion

This study proposed and evaluated a solution for 5G-NR V2X Sidelink (SL) to support URLLC at 5.9GHz. Our proposed concept consists of applying a 5G NR numerology-3, a 5G-NR V2X mode 2(c) deterministic scheduler and an analytical V2X SL URLLC admission control mechanism. We demonstrated that 5G NR V2X SL can achieve a reliability of 10^{-4} at a latency lower than 1 ms with reliability of 10^{-1}. Although such URLLC performance is limited to a group of fewer than 10 vehicles in 300-byte packets, it is a reasonable density for a 5G-NR V2X SL URLLC service. In future work, we plan to extend our analytical admission control algorithm to include more realistic mobility and channel conditions, and apply ML/AI mechanisms to better adapt the mode 2(c) scheduler to dynamic environments.

Acknowledgment

This work has received funding from the European Union's Horizon 2020 R&D program under grant agreement No: 101015405 for Safe4RAIL-3 (https://safe4rail-3.eu/) and No: 957218 for Intelliot (https://intelliot.eu/).

References

[1] M. H. C. Garcia, A. Molina-Galan, M. Boban, J. Gozalvez, B. Coll-Perales, T. Şahin, and A. Kousaridas, "A Tutorial on 5G NR V2X Communications," *IEEE Communications Surveys Tutorials*, vol. 23, no. 3, pp. 1972–2026, 2021.

[2] R. Ali, Y. B. Zikria, A. K. Bashir, S. Garg, and H. S. Kim, "URLLC for 5G and Beyond: Requirements, Enabling Incumbent Technologies and Network Intelligence," *IEEE Access*, vol. 9, pp. 67 064–67 095, 2021.

[3] D. Segura, E. J. Khatib, J. Munilla, and R. Barco, "5G Numerologies Assessment for URLLC in Industrial Communications," *Sensors*, vol. 21, p. 2489, 04 2021.

[4] M. Zambianco and G. Verticale, "Mixed-Numerology Interference-Aware Spectrum Allocation for eMBB and URLLC Network Slices," in *2021 19th Mediterranean Communication and Computer Networking Conference (MedComNet)*, 2021, pp. 1–8.

[5] L. Feng, W. Li, Y. Lin, L. Zhu, S. Guo, and Z. Zhen, "Joint Computation Offloading and URLLC Resource Allocation for Collaborative MEC Assisted Cellular-V2X Networks," *IEEE Access*, vol. 8, pp. 24 914–24 926, 2020.

[6] X. Ge, "Ultra-Reliable Low-Latency Communications in Autonomous Vehicular Networks," *IEEE Transactions on Vehicular Technology*, vol. 68, no. 5, pp. 5005–5016, 2019.

[7] L. Gallo and J. Härri, "Unsupervised Long- Term Evolution Device-to-Device: A Case Study for Safety-Critical V2X Communications," *IEEE Vehicular Technology Magazine*, vol. 12, no. 2, pp. 69–77, 2017.

[8] ETSI, "5G;NR;Study on Scenarios and Requirements for Next Generation Access Technologies," *3GPP TR 38.913 version 17.0.0 Release 17*, 2022-03.

[9] P. Popovski, Stefanović, J. J. Nielsen, E. de Carvalho, M. Angjelichinoski, K. F. Trillingsgaard, and A.-S. Bana, "Wireless Access in Ultra-Reliable Low-Latency Communication (URLLC)," *IEEE Transactions on Communications*, vol. 67, no. 8, pp. 5783–5801, 2019.

[10] K. B. Shashika Manosha, S. K. Joshi, M. Codreanu, N. Rajatheva, and M. Latva-aho, "Admission Control Algorithms for QoS-Constrained Multicell MISO Downlink Systems," *IEEE Transactions on Wireless Communications*, vol. 17, no. 3, pp. 1982–1999, 2018.

[11] N. U. Ginige, K. B. Shashika Manosha, N. Rajatheva, and M. Latva-aho, "Admission Control in 5G Networks for the Coexistence of eMBB-URLLC Users," in *2020 IEEE 91st Vehicular Technology Conference (VTC2020-Spring)*, 2020, pp. 1–6.

[12] J. Yan and J. Härri, "MCS Analysis for 5G-NR V2X Sidelink Broadcast Communication," in *IEEE 33rd Intelligent Vehicles Conference*, 2022. In process.

[13] ETSI, "5G NR; Physical layer procedures for data," *3GPP TS 38.214 version 16.2.0 Release 16*, 2020-07.

[14] L. Gallo and J. Härri, "Short paper: A LTE-direct Broadcast Mechanism for Periodic Vehicular Safety Communications," in *2013 IEEE Vehicular Networking Conference*, 2013, pp. 166–169.